EUROPEAN ORGANISATION FOR NUCLEAR RESEARCH

CERN-EP/88-29
March 4th, 1988

Production of low transverse energy clusters in $\bar{p}p$ collisions at $\sqrt{s} = 0.2 - 0.9$ TeV and their interpretation in terms of QCD jets.

UA1 Collaboration, CERN, Geneva, Switzerland

Aachen[1] - Amsterdam (NIKHEF)[2] - Annecy (LAPP)[3] - Birmingham[4] - CERN[5] - Harvard[6] - Helsinki[7] - Kiel[8] - Imperial College, London[9] - Queen Mary College, London[10] - Madrid (CIEMAT)[11] - MIT[12] - Padua[13] - Paris (College de France)[14] - Riverside[15] - Rome[16] - Rutherford Appleton Lab[17] - Saclay (CEN)[18] - Victoria[19] - Vienna[20] - Wisconsin[21] Collaboration

C. Albajar[5], M.G. Albrow[17], O.C. Allkofer[8], A. Astbury[19], B. Aubert[3], T. Axon[9], C. Bacci[16], T. Bacon[9], N. Bains[4], J. R. Batley[10], G. Bauer[6], S. Beingessner[19], A. Bettini[13], A. Bezaguet[5], R. Bonino[4], K. Bos[2], E. Buckley[6], G. Busetto[13], P. Catz[3], P. Cennini[5], S. Centro[13], F. Ceradini[16], D.G. Charlton[4], G. Ciapetti[16], S. Cittolin[5], D. Clarke[10], D. Cline[21], C. Cochet[18], J. Colas[3], P. Colas[18], M. Corden[4], J.A. Coughlan[17], G. Cox[4], D. Dau[8], J.P. deBrion[18], M. DeGiorgi[13], M. Della Negra[5], M. Demoulin[5], D. Denegri[5,18], A. DiCiaccio[5,16], F.J. Diez Hedo[11], L. Dobrzynski[14], J. Dorenbosch[2], J. D. Dowell[4], E. Duchovni[5], K. Eggert[1], E. Eisenhandler[10], N. Ellis[4], P. Erhard[1], H. Faissner[1], I.F. Fensome[10], A. Ferrando[11], M. Fincke-Keeler[19], P. Flynn[17], G. Fontaine[14], J. Garvey[4], D. Gee[15], S. Geer[6], A. Geiser[1], C. Ghesquiere[14], P. Ghez[3], C. Ghiglino[3], Y. Giraud-Heraud[14], A. Givernaud[5,18], A. Gonidec[5], H. Grassmann[1], J. Gregory[4], W. Haynes[17], S.J. Haywood[4], D.J. Holthuizen[2], M. Ikeda[15], W. Jank[5], M. Jimack[4], G. Jorat[5], D. Joyce[15], P.I.P. Kalmus[10], V. Karimäki[7], R. Keeler[19], I. Kenyon[4], A. Kernan[15], A. Khan[9], W. Kienzle[5], R. Kinnunen[7], M. Krammer[20], J. Kroll[6], D. Kryn[14], F. Lacava[16], M. Landon[10], J.P. Lees[3], R. Leuchs[8], S. Levegrün[8], S. Li[19], M. Lindgren[15], D. Linglin[3], P. Lipa[20], E. Locci[5], T. Markiewicz[21], C. Markou[9], M. Markytan[20], M.A. Marquina[11], G. Maurin[5], J.-P. Mendiburu[14], A. Meneguzzo[13], J. P. Merlo[15], T. Meyer[5], M.-N. Minard[3], M. Mohammadi[21], K. Morgan[15], M. Moricca[16], H.-G. Moser[1], A. Moulin[1], B. Mours[3], Th. Muller[5], L. Naumann[5], P. Nedelec[14], A. Nisati[16], A. Norton[5], G. Pancheri[6], F. Pauss[5], C. Perault[3], E. Petrolo[16], G. Piano Mortari[16], E. Pietarinen[7], C. Pigot[18], M. Pimiä[7], A. Placci[5], J.-P. Porte[5], M. Preischl[8], E. Radermacher[5], T. Redelberger[1], H. Reithler[1], J.-P. Revol[12], D. Robinson[9], T. Rodrigo[11], J. Rohlf[6], P. Rossi[13], C. Rubbia[5], G. Sajot[14], G. Salvini[16], J. Sass[5], D. Samyn[5], D. Schinzel[5], M. Schröder[8], A. Schwartz[6], W. Scott[17], C. Seez[9], T. P. Shah[17], I. Sheer[15], I. Siotis[9], D. Smith[15], R. Sobie[19], P. Sphicas[12], J. Strauss[20], J. Streets[4], C. Stubenrauch[18], D. Summers[21], K. Sumorok[6], F. Szoncso[20], C. Tao[14], A. Taurok[20], I. ten Have[2], S. Tether[12], G. Thompson[10], E. Tscheslog[1], J. Tuominiemi[7], W. van de Guchte[2], A. van Dijk[2], B. van Eijk[2], J.P. Vialle[3], L. Villasenor[21], T.S. Virdee[9], W. von Schlippe[10], J. Vrana[14], V. Vuillemin[5], K. Wacker[1], G. Walzel[20], A. Wildish[9], I. Wingerter[3], S. J. Wimpenny[5], X. Wu[12], C.-E. Wulz[20], T. Wyatt[5], M. Yvert[3], C. Zaccardelli[16], I. Zacharov[2], N. Zaganidis[18], L. Zanello[16] and P. Zotto[13].

(Submitted to Nucl. Phys. B)

ABSTRACT

The production of transverse energy clusters in minimum bias proton-antiproton collisions at the CERN SPS Collider is studied with the UA1 detector over a new range of centre of mass energies ($\sqrt{s}$ = 0.2 – 0.9 TeV). This study is intended to investigate how low in transverse momentum perturbative QCD is able to describe the dynamics of hadron collisions. We observe that clusters with transverse energy in excess of few GeV exhibit properties in agreement with QCD expectations for parton scattering, supporting their interpretation in terms of jet production. We find that the jet-event rate represents a sizeable fraction of the inelastic rate and is increasing with $\sqrt{s}$ over the measured energy range.

1. Introduction.

The production of hadronic jets at the SPS Collider and at the ISR has been clearly demonstrated by selecting events with large total transverse energy, ΣE_T, of all particles emitted in a given central rapidity interval, $\Delta\eta$, over the full azimuthal angle, $\Delta\phi = 2\pi$ [1]. There is now little doubt that high p_T jets are the observable result of a hard scattering between the hadron constituents, partons, and that the direction and energy of the jets (defined by a suitable algorithm) provide a good measurement of the emitted partons. As ΣE_T decreases, one reaches a regime where the interpretation of the event toplogy becomes more difficult. There can be several reasons for this: i) multiple parton-parton interactions [2], ii) an increasing relative contribution to the transverse energy from gluon radiation as the momentum transfer, Q^2, decreases [3], iii) an increasing relative contribution from events of high multiplicity, without evident jet production, that can produce large ΣE_T.

The cross-over value in ΣE_T, above which jets are observed to dominate, depends on $\sqrt{s}$ and on the chosen rapidity interval $\Delta\eta$ [4]. For example at $\sqrt{s} = 630$ GeV, for $\Delta\eta \simeq 2$ the cross–over occurs at about 60 GeV [5], for $\Delta\eta \simeq 6$ it occurs above 180 GeV [3]. These high cross-over values imply that ΣE_T triggers over $\Delta\phi = 2\pi$ are not suitable to study hadronic jets with small transverse energy. In order to extend the study of jet production at low energies it is necessary to use a localized E_T trigger rather than a global ΣE_T trigger. Previous studies [6] have shown that an appropriate solid angle is in the region $\Delta R = \sqrt{(\Delta\eta^2 + \Delta\phi^2)} \simeq 1$. It is then interesting to investigate whether the transverse energy clusters selected in this way behave as expected for QCD jets even at low values of E_T.

In this paper we present a study of the properties of clusters selected by the UA1 jet finding algorithm [6] down to the smallest possible threshold value. This study is applied to minimum bias trigger data, collected in the centre of mass energy range $\sqrt{s} = 0.2 - 0.9$ TeV; this extended energy range was made possible by the successful operation of the SPS $\bar{p}p$ Collider in pulsed mode [7].

The two main limitations that have to be taken into account when dealing with low transverse energy jets are that :

i) the experimental definition of a jet, rather clear at high E_T, becomes less reliable when the scattered parton E_T is not large with respect to the contribution from the "underlying event" (*i.e.* the contribution from the spectators and initial state bremsstrahlung);

ii) at low E_T values it becomes more difficult to describe parton-parton collisions by QCD perturbative calculations and the direct identification of partons with jets may be questioned [8].

The purpose of this investigation [9] is to determine how the measured cross section for clusters of $E_T > E_{Tmin}$ compares with QCD calculations. We shall present evidence that one can usefully define jets down to $E_{Tmin} \simeq 5$ GeV and that the QCD calculated and experimental cross sections agree over a very wide range of $E_T > E_{Tmin}$. As stressed in points i) and ii) above, the interpretation of the production of low E_T clusters in $\bar{p}p$ collisions in terms of QCD jets cannot be unique. Anyway an analysis of transverse energy clusters, as defined by our jet finding algorithm, can be a clear quantitative point of reference also for alternative interpretations. On the other hand, we must recall that jets have been defined in e^+e^- collisions down to energies as low as a few GeV and that the spin of the quark was determined from the jet axis angular distribution at $\sqrt{s}$=7 GeV [10].

In Sec.2 we present the event selection criteria and give a description of the UA1 jet finding algorithm. Sec.3 is devoted to the analysis of the properties of the clusters reconstructed by the algorithm: shape, angular distributions and production rate. In Sec.4 we discuss the corrections that we apply to the energy and rate of the clusters to account for the jet fragmentation, the algorithm selection and the experimental resolution. After that we derive the inclusive cross section that can be compared with QCD calculations. Results on the rate of events with low transverse energy clusters are presented in Sec. 5.

2. Data sample and selection criteria.

The SPS Collider was operated in pulsed mode between beam momenta of 100 and 450 GeV/c. The cycle was of 21.6 seconds with a flat top of 4.0 s, a flat bottom of 8.2 s and two energy ramps of 4.7 s each. The UA1 detector has been extensively described [11]. Its main characteristics are full solid angle calorimetric coverage and a charged particle tracking chamber, C.D., in a dipole magnet. The detector was triggered through all of the SPS cycle requiring at least two charged particles in opposite rapidity hemispheres in the range $1.5 < |\eta| < 5.5$. This trigger [12] accepts almost all of the inelastic non diffractive cross section. The trigger cross section at $\sqrt{s}$ =

546 GeV is derived from measurements of the total interaction rate [13], the data at all other energies are normalized to that energy since the Collider luminosity was proportional to the beam momentum [7]. It should be noted that, when comparing data taken at different c.m. energies, most of the systematic effects due to the detector response and to the beam parameters cancel, since the data were taken with the same circulating beams and in the same experimental conditions.

The present analysis is based on 188000 events collected during the Pulsed Collider run in March 1985, 18 % at flat bottom, $\sqrt{s} = 0.2$ TeV, and 34 % at flat top, $\sqrt{s} = 0.9$ TeV, while 48 % of the events were taken in the energy ramps and have been subdivided for the analysis into five c.m. energy intervals roughly equispaced in ln s. The total integrated luminosity was 5.1 μb^{-1}. A sample of 41000 minimum bias events at $\sqrt{s} = 546$ GeV and 66000 events at $\sqrt{s} = 630$ GeV collected during the 1983 and 1984 Collider runs respectively, are used to compare minimum bias and jet trigger data under the same experimental conditions.

Events are retained for analysis if they fulfil requirements on timing of the trigger hodoscopes, on the vertex reconstruction by the C.D. and on the total energy deposited in the calorimeter. With these cuts the residual background due to beam-gas interactions and halo particles was less than 2 %, while the efficiency for selecting $\bar{p}p$ non-diffractive interactions was higher than 96 %.

Clusters are defined by the UA1 jet finding algorithm [6] which is based on calorimeter transverse energy depositions in $\eta-\phi$ space. Calorimeter cells with E_T larger than 1.5 GeV are used to initiate a jet. The E_T deposited within a distance $\Delta R = \sqrt{(\Delta\eta^2 + \Delta\phi^2)} = 1$ is associated to the jet initiators. The cluster energy and axis are defined by the vector sum of all energy depositions in the cone of radius $\Delta R = 1$. In the following, E_T^{raw} refers to the transverse energy as reconstructed by the algorithm. Clusters are considered only if their axis is in the pseudorapidity interval $|\eta| < 1.5$ (central calorimeter) and have azimuth $|\Delta\phi| \geq 30°$ from the vertical where the two calorimeter halves join.

3. Analysis of cluster production. Can we consider them as low energy jets?

In a previous analysis [6] the properties of events containing high E_T jets were examined in terms of the transverse energy flow around the jet axis, $d^2E_T/d\Delta\eta d\Delta\phi$. We have shown that, for E_T

larger than 20 GeV, both the width of the jet and the transverse energy density outside the jet cone are roughly independent of the jet E_T. Using the present data sample we can now study the evolution of the properties of transverse energy clusters from the high E_T^{raw} region, where jet production is well understood in terms of hard parton scattering mechanism, down to very low values of E_T^{raw}.

Fig. 1 shows the transverse energy flow around the cluster axis, integrated over $\Delta\phi = \pm \pi/2$ from this axis, for different E_T^{raw} thresholds at $\sqrt{s} = 630$ GeV. From 60 GeV down to events with E_T^{raw} larger than 5 GeV the cluster profile is broad, with a base–width of the cluster that remains rather constant. At lower values of E_T^{raw} the cluster profile becomes narrow due to the bias of the algorithm that requires an initiator of $E_T \geq 1.5$ GeV. At low E_T the cluster width is essentially the size of a calorimeter cell.

To study the shape of low transverse energy clusters we have plotted the ratio, F, between the E_T contained in a cone of radius $\Delta R = 0.2$, comparable with the size of the calorimeter cells, and the E_T contained in the cone of radius $\Delta R = 1$. Fig. 2a shows the distribution of the average value of F, $\langle \Sigma E_T(\Delta R{=}0.2) / \Sigma E_T(\Delta R{=}1) \rangle$, as a function of E_T^{raw} for minimum bias and jet trigger data at $\sqrt{s} = 630$ GeV. As the transverse energy of the cluster increases, $\langle F \rangle$ shows a fast decrease from the initiator threshold, where F = 1. For $E_T^{raw} > 5$ GeV, $\langle F \rangle$ flattens off and then increases up to the high E_T jet region. This increase is rather well reproduced with a QCD Monte Carlo [14] and it is due to the limited transverse momentum of the fragments around the jet axis.

Events containing high E_T jets are also characterized by a transverse energy outside the jet cone [6] larger than the average value measured in minimum bias events. Fig. 2b shows the behaviour of the transverse energy density, $dE_T/d\eta$, measured in $\Delta\phi = \pm \pi/2$ around the cluster axis and at $\Delta\eta = 1.5$ from the cluster axis, as a function of E_T^{raw} for minimum bias and jet trigger data at $\sqrt{s} = 630$ GeV. The transverse energy density shows an increase from the average value measured in minimum bias events, that is about 1.5 GeV per unit of pseudorapidity in $\Delta\phi = \pi$, and tends to flatten off for $E_T^{raw} > 15$ GeV.

To check that the observed clusters are not an artefact of our calorimeter, we have studied the charged particle average transverse momentum flow around the cluster axis for $E_T^{raw} > 5$ GeV using the C.D. which has a far better space resolution. We observe clusters with similar shapes both in pseudorapidity and azimuthal angle (see Fig. 3).

We now examine the angular correlations between clusters. At $\sqrt{s} = 900$ GeV, in the sample of events containing at least one cluster in $|\eta| < 1.5$ and with $E_T^{raw} > 5$ GeV, we find that 34.4 % of the events contain a second cluster selected with the same criteria. The QCD Monte Carlo [14] prediction at $\sqrt{s} = 900$ GeV is 35.9 %. The absolute value of this fraction, f, is very sensitive to the efficiency of finding a second, lower E_T, jet. This efficiency depends on the E_T threshold and also on $\sqrt{s}$ through the influence of the transverse energy density in the underlying event. If corrections are applied for these effects, we find that f is roughly independent of both E_T^{raw} and $\sqrt{s}$, as expected for jet production. We have already shown [15] that the angular distribution for high E_T jet pairs is rather independent of the two-jet invariant mass, M, in good agreement with QCD which predicts only slow variations due to non–scaling effects. The angular distribution, $(1/N)dn/d\cos\theta$, of the two highest E_T clusters in their centre of mass system, is shown in Fig. 4a for different mass thresholds and compared to a leading order QCD prediction. The two-cluster $\Delta\phi$ distribution is shown in Fig. 4b together with QCD Monte Carlo predictions. The agreement with QCD is satisfactory for $M > 20$ GeV/c^2 corresponding to about $E_T^{raw} > 7.5$ GeV.

We now discuss which fraction of the reconstructed clusters can be attributed to QCD jets rather than to transverse energy fluctuations in soft collisions. In ref.5 UA2 extracted a parametrisation for the soft and hard cross-sections directly from the data. Over the pseudorapidity interval $|\eta| < 1$, their parametrisation is such that the hard cross–section prevails over the soft cross–section for $\Sigma E_T \geq 60$ GeV. For a two cluster inclusive cross-section of total transverse energy $\hat{E}_T = E_{T1} + E_{T2}$ (E_{T1} and E_{T2} are the transverse energies of the two highest E_T clusters produced in $|\eta| < 1$), the same parametrisation predicts that the cross–over in $\hat{E}_T$ occurs at $\hat{E}_T \simeq 25$ GeV. The UA2 analysis indicates that clusters with $E_T \leq 15$ GeV are mostly due to fluctuations of the soft component.

This conclusion is based on a phenomenological parametrisation of the hard cross–section that is not derived from QCD. To describe the hard cross section, the experimental distribution, $dn/d\hat{E}_T$, was extrapolated below 65 GeV by an exponential in $\hat{E}_T$ joining smoothly with the large $\hat{E}_T$ data [5]. Fig. 5 shows the event yield as a function of $\hat{E}_T$ for the UA2 and the UA1 experiment. For comparison, the UA1 data are analysed in the restricted pseudorapidity range $|\eta| < 1$. Although they are obtained with a different calorimeter and cluster algorithm, the two sets of data are in good agreement. This is also shown in Fig. 6, where the fraction of the transverse energy contained in the two highest E_T clusters, $h_1 = E_{T1} / \Sigma E_T$, $h_2 = (E_{T1} + E_{T2}) / \Sigma E_T$, is plotted as a function of $\hat{E}_T$.

The two lines shown in Fig. 5 are the UA2 parametrisation for the hard cross–section (dashed line), with its extrapolation by an exponential below 65 GeV, and the ISAJET [14] absolute QCD prediction (full line). If we replace the phenomenological UA2 parametrisation of the hard cross–section by the ISAJET prediction, we conclude that the observed cluster yield is consistent with a QCD model down to values of the transverse energy smaller than 15 GeV.

At low $\hat{E}_T$ values QCD predicts that in more than 70 % of the cases only one of the two clusters is emitted in the central rapidity interval $|\eta| < 1$. The $\hat{E}_T$ variable was discussed for the purpose of comparison with UA2, but it is more appropriate to discuss our single inclusive cluster yield as a function of the cluster E_T. We compare this yield with the predictions of two different phenomenological parametrisations of the minimum bias inelastic $\bar{p}p$ collisions.

Fig. 7 shows the uncorrected cluster yield as a function of E_T^{raw} in $|\eta| < 1.5$ at $\sqrt{s} = 0.9$ TeV. The solid lines are the predictions of a minimum bias event generator [16] based on longitudinal phase space hadronization of the spectators. The Monte Carlo generated events have been fully simulated in the detector, and then processed and analysed in the same way as real events. The clusters reconstructed by this Monte Carlo mainly originate in large multiplicity events. We see that transverse energy fluctuations from soft collisions account for only 18% of the cluster yield for $E_T^{raw} > 5$ GeV and that the E_T distribution is much steeper than for the data. It is interesting to investigate whether "non QCD" event generators based on cluster emission [19, 20] are able to produce cluster yields comparable to our measurements. These Monte Carlo event generators introduce a number of phenomenological assumptions based on the characteristics of the minimum bias $\bar{p}p$ collisions as measured by the Collider experiments. In Fig. 7 we show the results of the reconstruction in our apparatus of events generated with the UA5 cluster Monte Carlo [21] at $\sqrt{s} = 0.9$ TeV (dashed lines). The cluster yield is still too low to account for the measured distribution.

This and other [22] statistical models, based on phenomenological assumptions, are able to reproduce some of the features of the production of low E_T clusters. These models, though useful for a phenomenological approach, do not provide a description of the underlying dynamics of cluster production and cannot predict an absolute cross section.

Our aim in this paper is to investigate to what extent QCD, in its perturbative approach, can explain experimental results. The evidence presented above on the cluster shape, angular distribution and production rate suggests that the observed clusters with $E_T > 5$ GeV are consistent with having a substantial component of QCD jets. Of course we cannot assume from our results that a simple jet interpretation is unique when we go down to 5 GeV. This value does not represent any definite threshold for the onset of hard interactions. In fact hadronic interactions will evolve with continuity from low to high values of transverse energy; the 5 GeV cut used in this analysis represents a reasonable limit from where experimental results can be compared with QCD models. On this basis, we now proceed to compute the inclusive jet cross section.

4 . Inclusive jet cross section.

To derive the inclusive jet cross section, corrections are applied to the number of the reconstructed clusters and to the transverse energy recostructed by the algorithm.

First the yield of clusters has been corrected for the contribution from fluctuations of the transverse energy density as calculated with the minimum bias Monte Carlo [16].

As a second step, we relate the transverse energy reconstructed by the algorithm, E_T^{raw}, to the transverse energy of jets as modelled in QCD jet-event generators. We have used two different Monte Carlo programs, ISAJET [14] and COJETS [23], which give results in good agreement with each other. In the Monte Carlo the jet momentum is defined as the vector sum of the hadronic fragments of the parent parton(s) and it is compared with the energy reconstructed by the algorithm. Partons produced within a distance of $\Delta R = 0.75$ are merged in a single jet since the algorithm is not able to detect them as separate jets. Correction factors are derived at different c.m. energies to relate the cluster E_T^{raw} to the jet transverse momentum, p_T. Since available jet event generators do not reproduce well the rise of the transverse energy in the event as a function of E_T^{raw}, plotted in Fig. 2b, to derive this correction we have replaced bin by bin in the Monte Carlo the measured value of the transverse energy density.

The efficiency of the algorithm to find a jet of transverse momentum p_T is evaluated requiring that a cluster is reconstructed with its axis within an association distance $\Delta R_a = 0.75$ from the jet direction. The jet finding efficiency is about 55 % for $p_T = 5$ GeV/c and is higher than 90 % for $p_T = 10$ GeV/c.

The same procedure is used to evaluate the resolution function due to the fluctuations of the calorimeter energy response and of the jet finding algorithm. Averaging over the acceptance, the relative resolution for a 10 GeV/c transverse momentum jet is about 30 %. Finally the effect of the resolution function on the jet differential cross section is evaluated assuming a QCD leading order prediction [24] for the parent distribution .

We have checked that the result of the above corrections is stable with respect to small variations of the initiator threshold, from 1.35 to 1.65 GeV transverse energy, and of the association distance ΔR_a, from 0.65 to 0.9.

The inclusive jet cross section, $d^2\sigma/dp_T d\eta$, averaged over the range $|\eta| < 1.5$, is shown in Fig. 8 as a function of the jet p_T and compared with jet trigger data [26] for $\sqrt{s} = 546$ and 630 GeV. The systematic error, due to the jet energy scale and to the resolution function corrections, depends upon the jet p_T and is estimated to be a factor of two for $p_T \simeq 5$ GeV/c and a factor of 1.7 for p_T larger than 15 GeV/c. Also shown in the Fig. 8 is a QCD leading order calculation [24] obtained using the structure function parametrisation of ref.25 with $\Lambda_{QCD} = 0.2$ GeV and scale $Q^2 = p_T^2$. The theoretical prediction is scaled up by a factor of 1.5, as was done in ref.26, in order to agree with the experimental cross section for large transverse momentum jets, $p_T \simeq 60$ GeV/c. Perturbative QCD is expected to break down at low momentum transfer, moreover at low p_T its predictions depend strongly upon the behaviour of the gluon density at low x which is not measured directly but extrapolated from νN deep inelastic scattering data [27]. Nevertheless, the behaviour of the jet inclusive cross section, now measured over nine orders of magnitude, shows impressive agreement with perturbative QCD predictions within the systematic uncertainties.

Fig. 9a shows the jet inclusive cross section measured during the Pulsed Collider run at different c.m. energies. The same results are also given in Table 1. On average, the experimental data are a factor of two higher than leading order QCD predictions. As explained before, systematic uncertainties, both in the data and in the calculation, can account for part of this discrepancy. Most of the systematic errors cancel in the ratio of the inclusive cross section at different c.m. energies shown in Fig. 9b together with the QCD prediction. From 0.2 to 0.9 TeV c.m. energy, the inclusive jet cross section increases on average by a factor of about ten for $p_T \simeq 10$ GeV/c. The trend of the data indicates a rise of the cross section with $\sqrt{s}$, at fixed p_T, faster than foreseen by leading order QCD with the present choice of structure functions and Q^2 scale.

5 . Jet-event cross section.

The number of events containing at least one cluster with E_T larger than 5 GeV is used to evaluate a cross section due to hard processes. We define σ_{jet} as the cross section for producing at least one cluster with $E_T > 5$ GeV, as defined by our algorithm, at any rapidity. We measure it by searching for clusters in the restricted region $|\eta| < 1.5$ and then the cross section is corrected for the $|\eta| < 1.5$ acceptance using the Monte Carlo generated jet-events. This correction varies from 10 % at $\sqrt{s} = 0.2$ TeV to 32 % at $\sqrt{s} = 0.9$ TeV. Fig. 10 shows the jet-event cross section, σ_{jet}, as a function of the c.m. energy. The ± 20 % quoted systematic error accounts for the uncertainties in the background, efficiency and acceptance corrections. In the same figure we report results of the total $\bar{p}p$ cross section and of the inelastic non single diffractive cross section [28].

Attempts have been made [29], inspired by QCD, to model the low x parton scattering cross section at Collider and higher energies. The results depend strongly upon the parton transverse momentum threshold, p_T^{cut}, assumed in the calculation. The relation between the parton p_T and the jet transverse energy is experimentally poorly defined in this region due to uncertainties in the calorimeter energy scale, in the energy corrections and to smearing effects on the steeply falling E_T distribution. According to the Monte Carlo results, a nominal 5 GeV cut on the cluster transverse energy, as reconstructed by the algorithm, results in an effective average parton p_T threshold between 3 and 4 GeV/c. Moreover this effective threshold depends upon the c.m. energy. Predictions based on QCD [24, 30] for p_T^{cut} in the range 3 to 4 GeV/c give results compatible with the measurement, though they are very sensitive to the choice of the parameters, p_T^{cut}, Q^2 scale and to the behaviour of the structure functions at low x.

The jet-event cross section is rising from the ISR, where it is of order 10^{-1} mb [31], through the Pulsed Collider energy range up to about 18 mb when approaching 1 TeV c.m. energy, giving a sizeable contribution to the total $\bar{p}p$ cross section. The observed rise of the inelastic cross section may be associated with the increase of the jet-event cross section as suggested in ref.32.

6 . Conclusions.

We have analysed a sample of minimum bias trigger events collected with the UA1 dectector at the SPS Pulsed Collider from 0.2 to 0.9 TeV centre of mass energy.

A search for transverse energy clusters has shown that a substantial fraction of events contain at least one cluster with E_T larger than 5 GeV. These clusters exhibit characteristics similar to high E_T jets. The two cluster correlation in $\Delta\phi$ and $\cos\theta$ supports an interpretation in terms of hard parton scattering. The inclusive cluster yield is higher than foreseen by statistical models based on extrapolations of lower energy results.

Considering this evidence, we have extended the study of inclusive jet production in $\bar{p}p$ collisions from large transverse energies down to the low E_T region, $x_T=2E_T/\sqrt{s} \simeq 0.02$, and we have compared our results to perturbative QCD predictions. The agreement of the inclusive cross section with QCD over several orders of magnitude is quite remarkable. However with increasing c.m. energy the experimental data tend to be higher than the QCD predictions.

We have shown that the contribution of events with clusters to the inelastic non diffractive cross section becomes large when approaching 1 TeV c.m. energy and may be associated with the increase of the $\bar{p}p$ inelastic rate over the Pulsed Collider energy range.

QCD is able to account, within the limitations discussed in the text, for the production of clusters down to transverse energies in the region of 5-10 GeV. The understanding of these results in terms of low x parton scattering is relevant for future hadron colliders, in the multi–TeV region, where hard processes are expected to be an important source of the total inelastic rate.

Acknowledgments

We thank G. Altarelli, A. Silverman and J. Stirling for criticism and useful discussions. We are thankful to the management and staff of CERN and of all participating institutes for their vigorous support of the experiment. The following funding agencies have contributed to this programme:

Fonds zur Förderung der Wissenschaftlichen Forschung, Austria.
Valtion luonnontieteellinen toimikunta, Suomen Akatemia, Finland.
Institut National de Physique Nucléaire et de Physique des Particules and
Institut de Recherche Fondamentale (CEA), France.
Bundesministerium für Forschung und Technologie, Fed. Rep. Germany.
Istituto Nazionale di Fisica Nucleare, Italy.
Science and Engineering Research Council, United Kingdom.
Stichting Voor Fundamenteel Onderzoek der Materie, The Netherlands.
Department of Energy, USA.
The Natural Sciences and Engineering Research Council of Canada.

Thanks are also due to the following people who have worked with the collaboration in the preparations for and data collection on the runs described here: L.Baumard, F.Bernasconi, D. Brozzi, V.Cecconi, R.Conte, L.Dumps, G.Fetchenhauer, G.Gallay, J.C. Michelon and L.Pollet.

References

[1] M.Banner *et al.*: Physics Letters, **118B** (1982) 203.
G.Arnison *et al.*: Physics Letters, **123B** (1983) 115.
T.Akesson *et al.*: Physics Letters, **123B** (1983) 133.

[2] T.Akesson *et al.*: Zeitschrift fur Physik, **C34** (1987) 163.

[3] C.Albajar *et al.*: Zeitschrift fur Physik **C36** (1987) 33.

[4] T.Akesson and H.Bengtsson: Physics Letters, **120B** (1983) 233.

[5] J.A.Appel *et al.*: Physics Letters, **165B** (1985) 441

[6] G.Arnison *et al.*: Physics Letters, **132B** (1983) 214.

[7] R.Laukner: IEEE Transactions on Nuclear Science, **NS-32** (1985) 1653.

[8] A.H.Mueller: Proceedings of the 1985 International Symposium on Lepton and Photon Interactions at High Energies, Kyoto, August 1985, page 161 and references therein.

[9] L.V. Gribov, E.M.Levin and M.G.Ryskin: Physics Reports, **100** (1983) 1.
G.Pancheri and C.Rubbia: Nuclear Physics, **A418** (1984) 117.

[10] G.Hanson *et al.*: Physical Review Letters, **35** (1975) 1609.
San Lan Wu: Physics Reports, **107** (1984) 59.

[11] C.Cochet *et al.*: Nuclear Instruments Methods, **A243** (1986) 45.
B.Aubert *et al.*: Nuclear Instruments Methods, **176** (1980) 195; preprint LAPP-EXP-85-10
M.J.Corden *et al.*: Nuclear Instruments Methods, **A238** (1985) 273.
M.Calvetti *et al.*: IEEE Transactions Nuclear Science, **NS-30** (1983) 71.

[12] A.Astbury *et al.*: Nuclear Instruments Methods, **A238** (1985) 288.

[13] M.Bozzo *et al.*: Physics Letters, **147B** (1984) 392.
G.Arnison *et al.*: Physics Letters, **128B** (1983) 336.

[14] F.E.Paige and S.D.Protopopescu: ISAJET Version 5.20, BNL report 38034 (1986).

[15] G.Arnison *et al.*: Physics Letters, **177B** (1986) 244.

[16] F.E.Paige and S.D.Protopopescu: BNL report 31987 (1981). The M.C. reproduces the measured charged particle multiplicity at the different c.m. energies. The M.C. transverse momentum distribution does not depend upon the c.m. energy and its average value has been fixed to reproduce the $\langle p_T \rangle$ in low multiplicity events. In fact it has been observed [17,18] that this quantity is almost independent of the c.m. energy from the ISR to the SPS Collider.

[17] G.Arnison *et al.*: Physics Letters, **118B** (1982) 167.

[18] A.Breakstone *et al.*: Physics Letters, **132B** (1983) 463.

[19] D.Ward: Proceedings of the Workshop on Physics Simulation at High Energy, Madison, WI, May 1986, ed. V.Barger, T.Gottschalk and F.Halzen, World Scientific 1986, page 208.
G.J.Alner et al.: preprint CERN-EP/86-213, 1986, submitted to Nuclear Instruments and Methods.

[20] P.Aurenche, F.W.Bopp and J.Ranft: Proceedings of the Workshop on Physics Simulation at High Energy, Madison, WI, May 1986, ed. V.Barger, T.Gottschalk and F.Halzen, World Scientific 1986, page 193.

[21] This event generator, extensively described in ref.19, accounts for the measured charged particle multiplicity and transverse momentum distributions, the short range rapidity correlations and the dependence of the average transverse momentum with the event multiplicity [17]. We are grateful to David Ward who provided us with the UA5 Monte Carlo program.

[22] Chao Wei-qi, Meng Ta-chung and Pan Ji-cai: Physical Review Letters **58** (1987) 1399.

[23] R.Odorico: Computer Physics Communications, **32** (1984) 139.

[24] W.J.Stirling: Proceedings of the 6th Topical Workshop on $\bar{p}p$ Collider Physics, ed. K.Eggert, H.Faissner and E.Radermacher, World Scientific, page 301.

[25] D.W.Duke and J.F.Owens: Physical Review, **D30** (1984) 49.

[26] G.Arnison *et al.*: Physics Letters, **172B** (1986) 461.

[27] For a review of deep inelastic scattering data see M.Diemoz, F.Ferroni, E.Longo: Physics Reports, **130** (1986) 293.

[28] J.G.Rushbrooke: Proceedings of the 1985 International Europhyiscs Conference on High Energy Physics, ed. L.Nitti and G.Preparata, page 839 and references therein.
G.J.Alner *et al.*: Zeitschrift für Physik, **C33** (1986) 175.

[29] T.K.Gaisser and F.Halzen: Physical Review Letters, **54** (1985) 1754.
G.Pancheri and Y.Srivastava: Physics Letters, **159B** (1985) 69.

[30] G.Pancheri and Y.Srivastava: Physics Letters, **182B** (1986) 199.
A.Capella, J.Tran Thanh Van and J.Kwiecinski: Physical Review Letters **58** (1987) 2015.

[31] T.Akesson *et al.*: Physics Letters, **123B** (1983) 133.

[32] D.Cline, F.Halzen and J.Luthe: Physical Review Letters, **31** (1973) 491.
S.D.Ellis and M.B.Kislinger: Physical Review **D9** (1974) 2027.
L.Durand and Hong Pi: Physical Review Letters **58** (1987) 303.

[33] U.Amaldi *et al.*: Physics Letters, **66B** (1977) 390.

Figure captions

Fig.1 Transverse energy density around the cluster axis, with $\Delta\phi = \pm\ \pi/2$, for different E_T^{raw} thresholds from jet trigger (a,b) and minimum bias (c,d,e) data.

Fig.2 a) Average value of $F = \Sigma E_T(\Delta R{=}0.2) / \Sigma E_T(\Delta R{=}1)$ and b) transverse energy density, $dE_T/d\eta$ in $\Delta\phi = \pi$, away from the cluster axis (at $\Delta\eta = 1.5$) as a function of the cluster transverse energy, E_T^{raw} .

Fig.3 Average transverse momentum flow around the jet axis as a function of a) $\Delta\eta$ and b) $\Delta\phi$ at $\sqrt{s} = 0.9$ TeV, as resulting from tracks measured in the Central Detector.

Fig.4 Two-cluster angular distributions: a) $(1/N)dn/d\cos\theta$ for different mass thresholds, b) $(1/N)dn/d\Delta\phi$ for different E_T^{raw} thresholds.

Fig.5 Event yield as a function of $\hat{E}_T = E_{T1} + E_{T2}$. The corresponding results of UA2 are also given [5]. The dashed line is the UA2 parametrisation of the hard cross–section, the full line is the ISAJET [14] absolute prediction.

Fig.6 The ratio $h_1 = E_{T1}/\Sigma E_T$ (a) and $h_2 = (E_{T1} + E_{T2})/\Sigma E_T$ (b) as a function of $\hat{E}_T = E_{T1} + E_{T2}$. The corresponding results of UA2 are also given [5].

Fig.7 Inclusive cluster yield as a fuction of E_T^{raw} at $\sqrt{s} = 0.9$ TeV compared to a "minimum bias" Monte Carlo [16] (straight line) and results obtained by us using the UA5 random cluster Monte Carlo [19] (dashed line). The two lines define the statistical accuracy of the Monte Carlo calculations.

Fig.8 Inclusive jet cross section at $\eta = 0$ as a function of the jet p_T for a) $\sqrt{s} = 546$ GeV and b) $\sqrt{s} = 630$ GeV. The line is a QCD calculation [24] scaled up by a factor of 1.5.

Fig.9 a) Inclusive jet cross section at $\eta = 0$ for different values of $\sqrt{s}$. (See Table 1). The ISR data are from ref.31. The lines are QCD calculations [24] scaled up by a factor of 2.
b) Inclusive cross section ratios as a function of the jet p_T.

Fig.10 UA1 trigger cross section, σ_{trig}, and jet-event cross section, σ_{jet}, as a function of $\sqrt{s}$. Also shown are results on the $\bar{p}p$ total cross section and inelastic non single diffractive cross section. The full line is the σ_{tot} fit of ref.33, the dashed line is (2/3) σ_{tot}, the dot-dashed lines are from ref.30.

Table 1

Jet inclusive cross section

$\sqrt{s} = 200\ GeV$		$\sqrt{s} = 500\ GeV$		$\sqrt{s} = 900\ GeV$	
p_T (GeV/c)	$\left.\frac{d^2\sigma}{dp_T d\eta}\right\|_{\eta=0}$ $(\mu b\ GeV^{-1})$	p_T (GeV/c)	$\left.\frac{d^2\sigma}{dp_T d\eta}\right\|_{\eta=0}$ $(\mu b\ GeV^{-1})$	p_T (GeV/c)	$\left.\frac{d^2\sigma}{dp_T d\eta}\right\|_{\eta=0}$ $(\mu b\ GeV^{-1})$
5 − 6	119. ± 16.	5 − 6	275. ± 38.	5 − 6	482. ± 59.
6 − 7	56.3 ± 5.9	6 − 7	170. ± 18.	6 − 7	295. ± 25.
7 − 8	29.0 ± 2.8	7 − 8	105. ± 10.	7 − 8	180. ± 11.
8 − 9	12.0 ± 1.5	8 − 9	59.9 ± 6.6	8 − 9	116.0 ± 6.3
9 − 10	8.9 ± 1.2	9 − 10	37.5 ± 4.8	9 − 10	77.0 ± 4.1
10 − 11	4.51 ± 0.82	10 − 11	26.7 ± 3.9	10 − 11	61.1 ± 3.3
11 − 12	2.25 ± 0.57	11 − 12	14.7 ± 2.9	11 − 12	42.2 ± 2.6
12 − 14	1.17 ± 0.41	12 − 13	12.0 ± 2.6	12 − 13	33.5 ± 2.3
14 − 16	0.53 ± 0.20	13 − 14	9.1 ± 2.3	13 − 14	22.0 ± 1.8
16 − 22	0.10 ± 0.06	14 − 15	4.80 ± 0.17	14 − 15	18.4 ± 1.7
		15 − 17	3.93 ± 0.11	15 − 16	16.7 ± 1.6
		17 − 22	0.73 ± 0.33	16 − 18	10.5 ± 1.4
		22 − 29	0.27 ± 0.19	18 − 20	5.02 ± 0.96
				20 − 22	3.19 ± 0.78
				22 − 24	2.09 ± 0.65
				24 − 30	1.10 ± 0.47
				30 − 36	0.24 ± 0.10

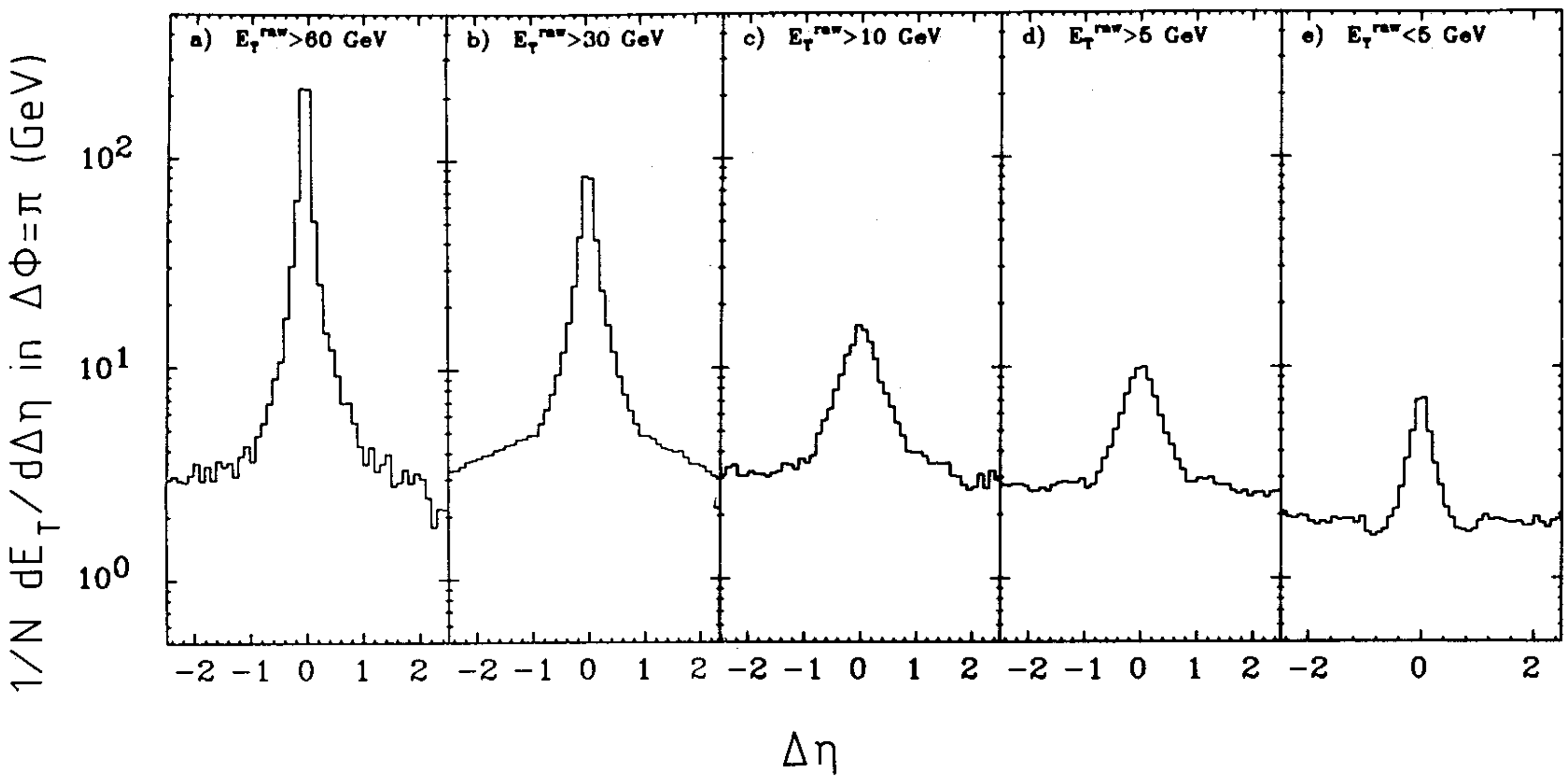
a) E_T^{raw}>60 GeV
b) E_T^{raw}>30 GeV
c) E_T^{raw}>10 GeV
d) E_T^{raw}>5 GeV
e) E_T^{raw}<5 GeV
1/N $dE_T/d\Delta\eta$ in $\Delta\Phi=\pi$ (GeV)
10^2
10^1
10^0
-2 -1 0 1 2
$\Delta\eta$

FIG. 1

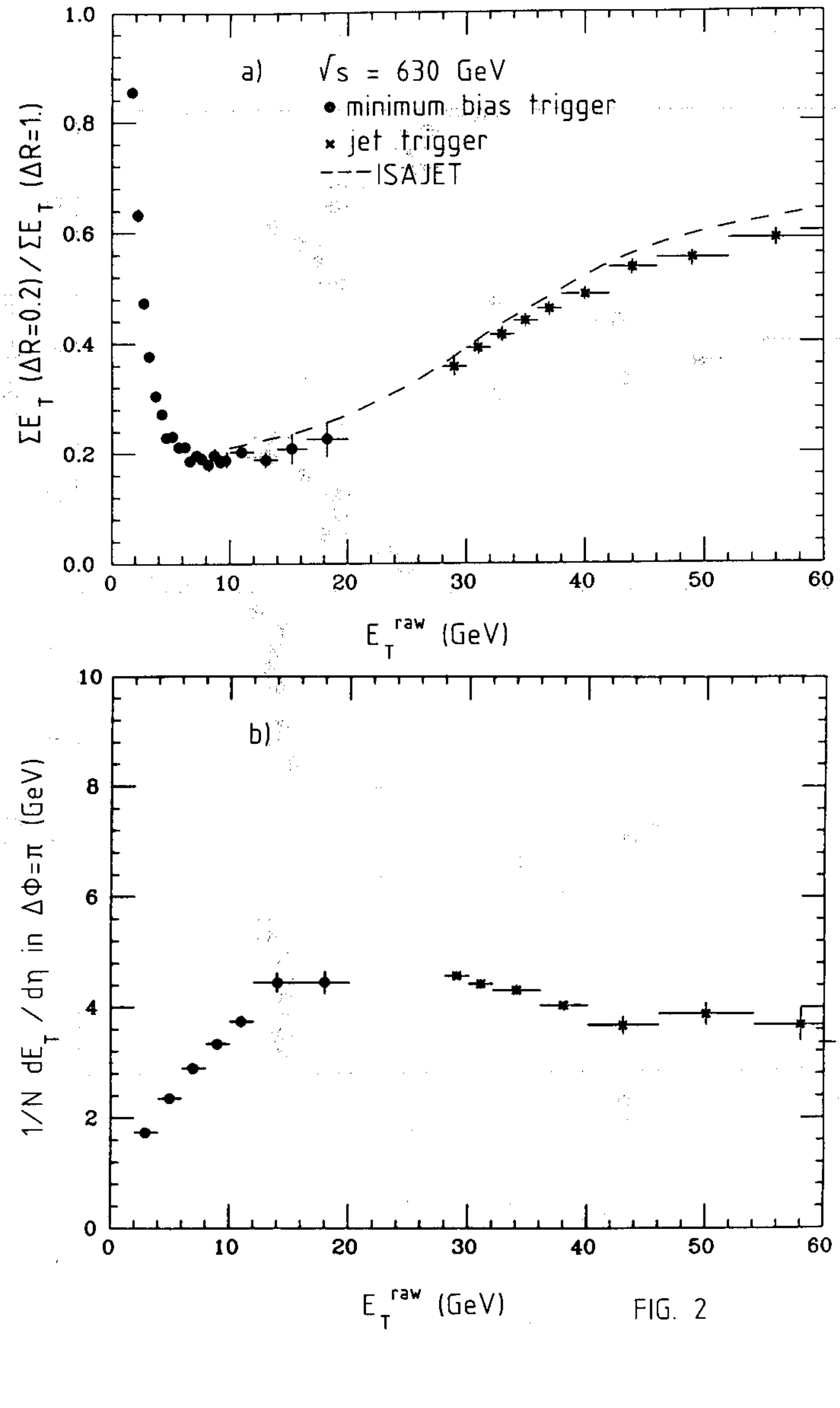

a)
√s = 630 GeV
minimum bias trigger
jet trigger
ISAJET
ΣE_T (ΔR=0.2) / ΣE_T (ΔR=1.)
E_T^raw (GeV)
b)
1/N dE_T / dη in ΔΦ=π (GeV)
E_T^raw (GeV)

FIG. 2

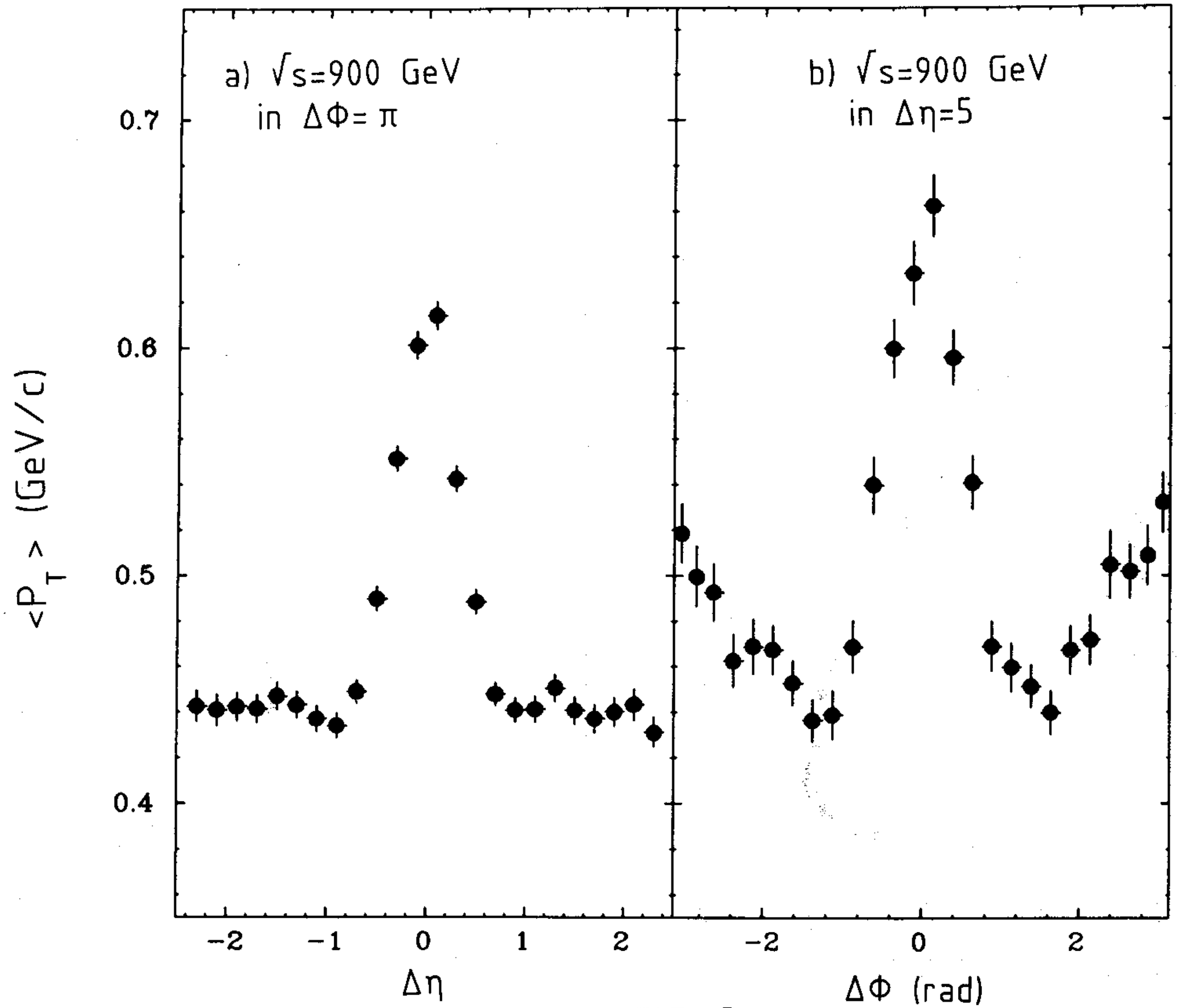
a) √s=900 GeV
in ΔΦ= π
b) √s=900 GeV
in Δη=5
<P_T> (GeV/c)
0.7
0.6
0.5
0.4
−2
−1
0
1
2
Δη
−2
0
2
ΔΦ (rad)

FIG. 3

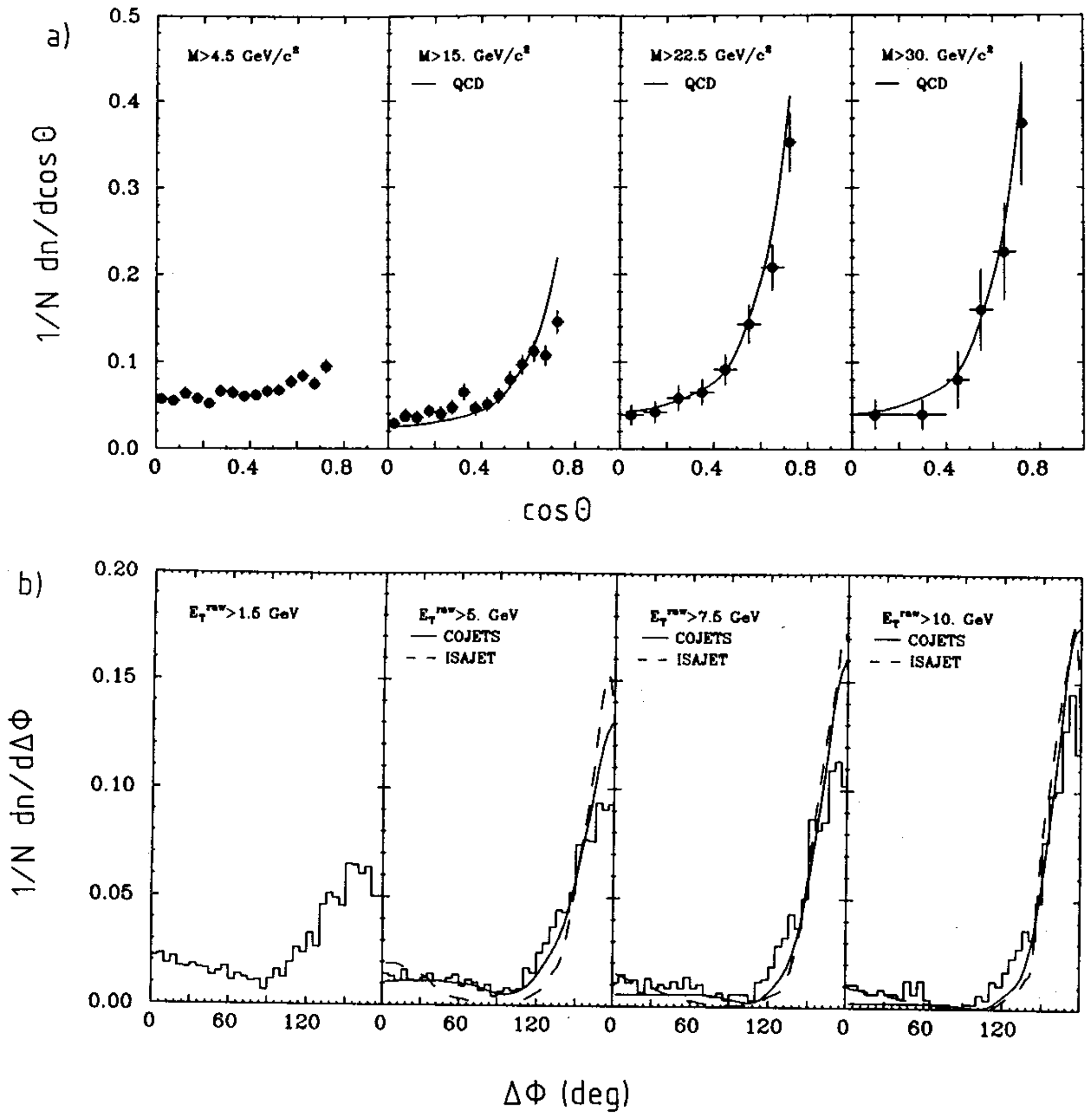
a)
1/N dn/dcos Θ
M>4.5 GeV/c²
M>15. GeV/c²
M>22.5 GeV/c²
M>30. GeV/c²
QCD
cos Θ
b)
1/N dn/dΔΦ
E_T^raw>1.5 GeV
E_T^raw>5. GeV
E_T^raw>7.5 GeV
E_T^raw>10. GeV
COJETS
ISAJET
ΔΦ (deg)

FIG. 4

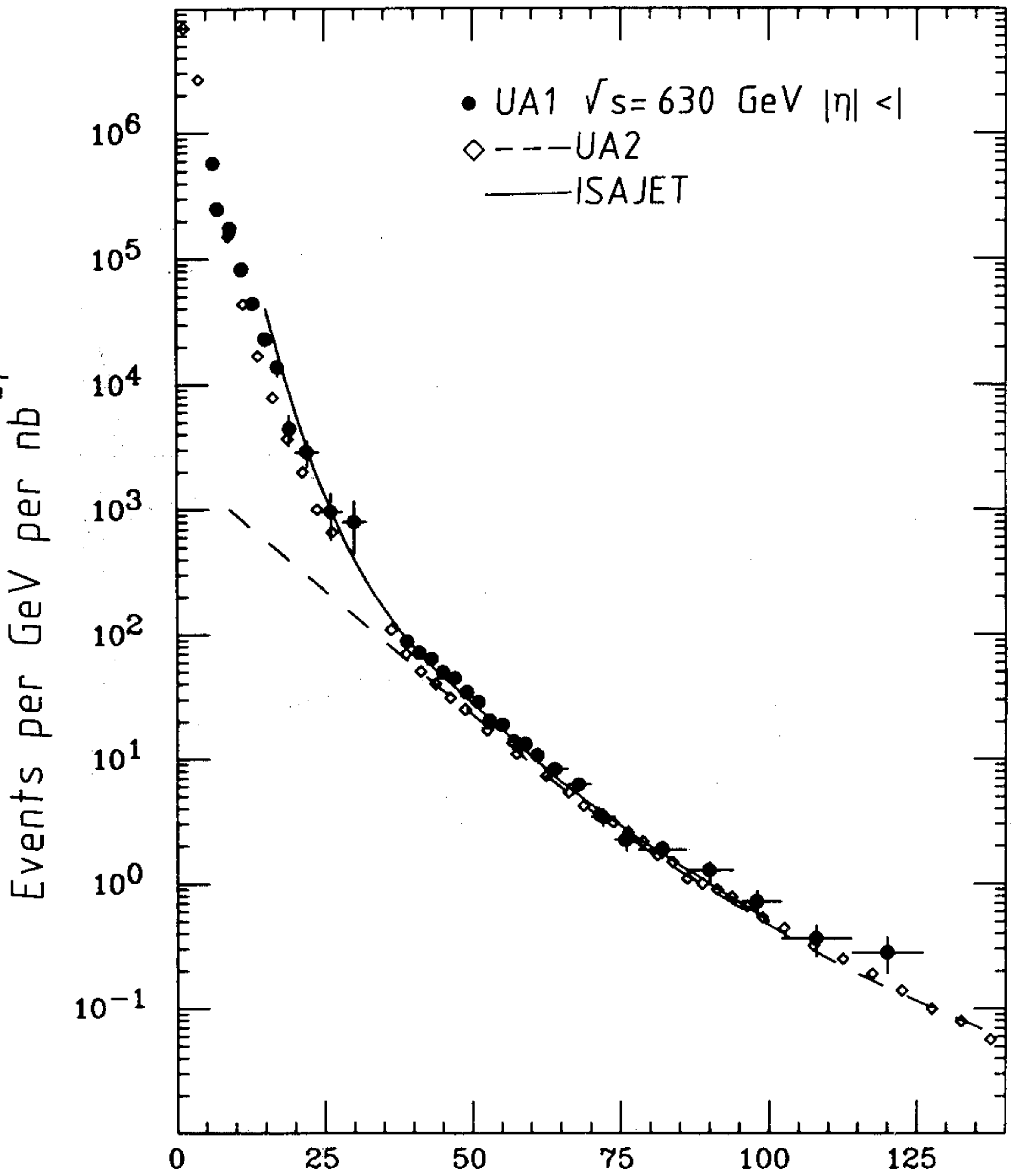

$\hat{E}_T = E_{T1} + E_{T2}$ (GeV)

FIG. 5

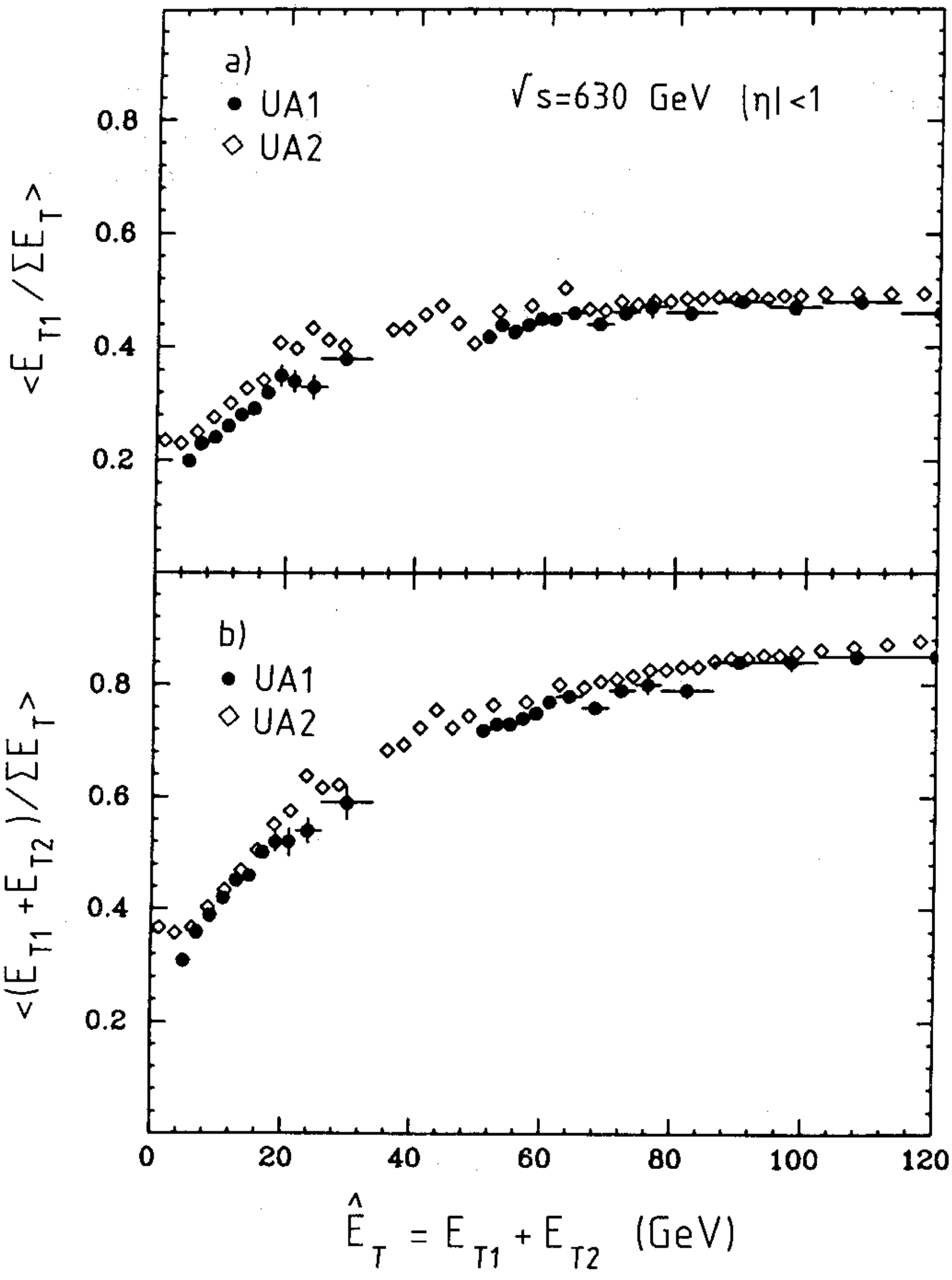
a)
UA1
UA2
√s=630 GeV |η|<1
0.8
0.6
0.4
0.2
<E_T1 /ΣE_T>
b)
UA1
UA2
0.8
0.6
0.4
0.2
<(E_T1 +E_T2)/ΣE_T>
0
20
40
60
80
100
120
Ê_T = E_T1 + E_T2 (GeV)

FIG. 6

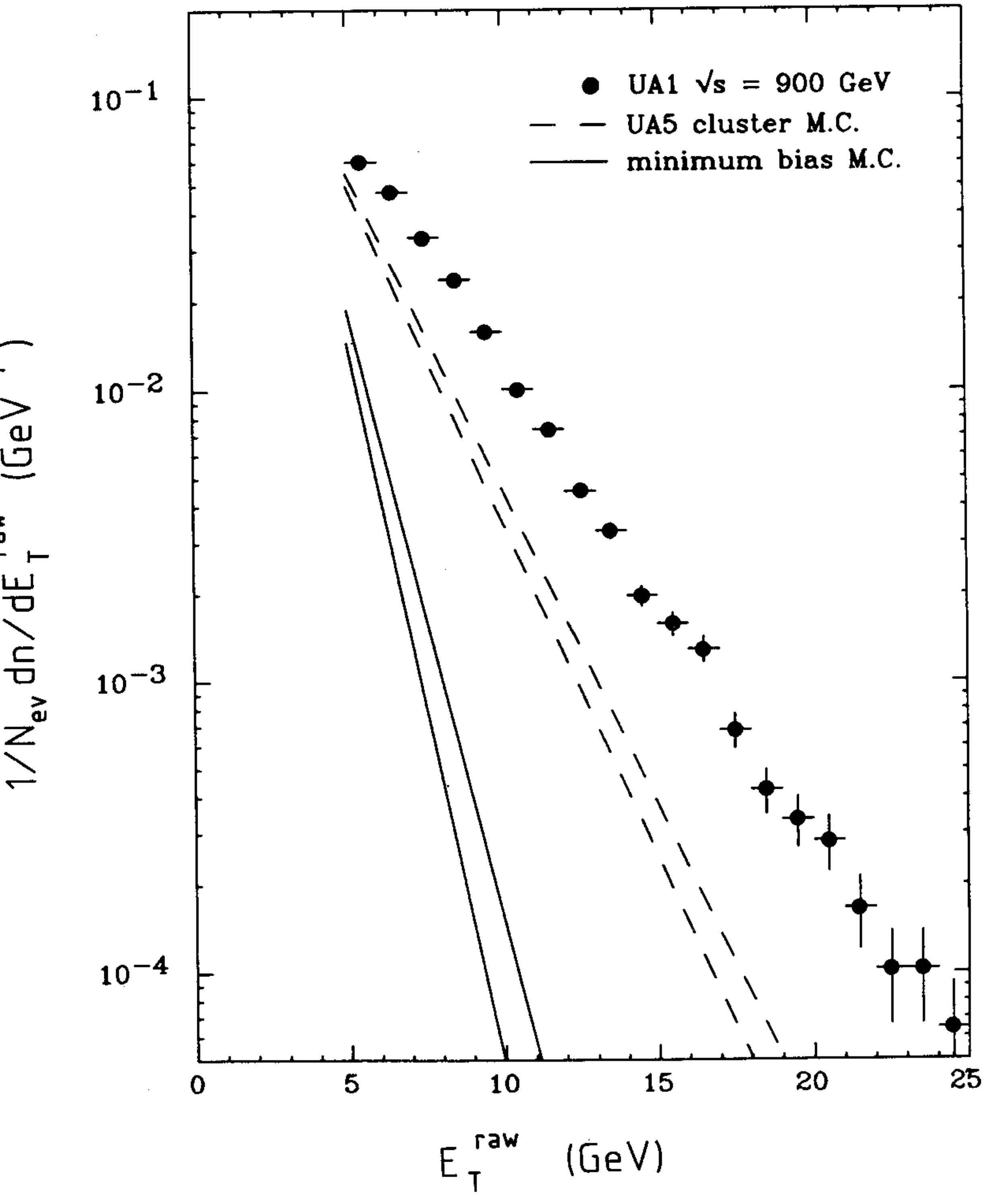

UA1 √s = 900 GeV
UA5 cluster M.C.
minimum bias M.C.
10^{-1}
10^{-2}
10^{-3}
10^{-4}
$1/N_{ev}\, dn/dE_T^{raw}$ (GeV^{-1})
0
5
10
15
20
25
E_T^{raw} (GeV)

FIG. 7

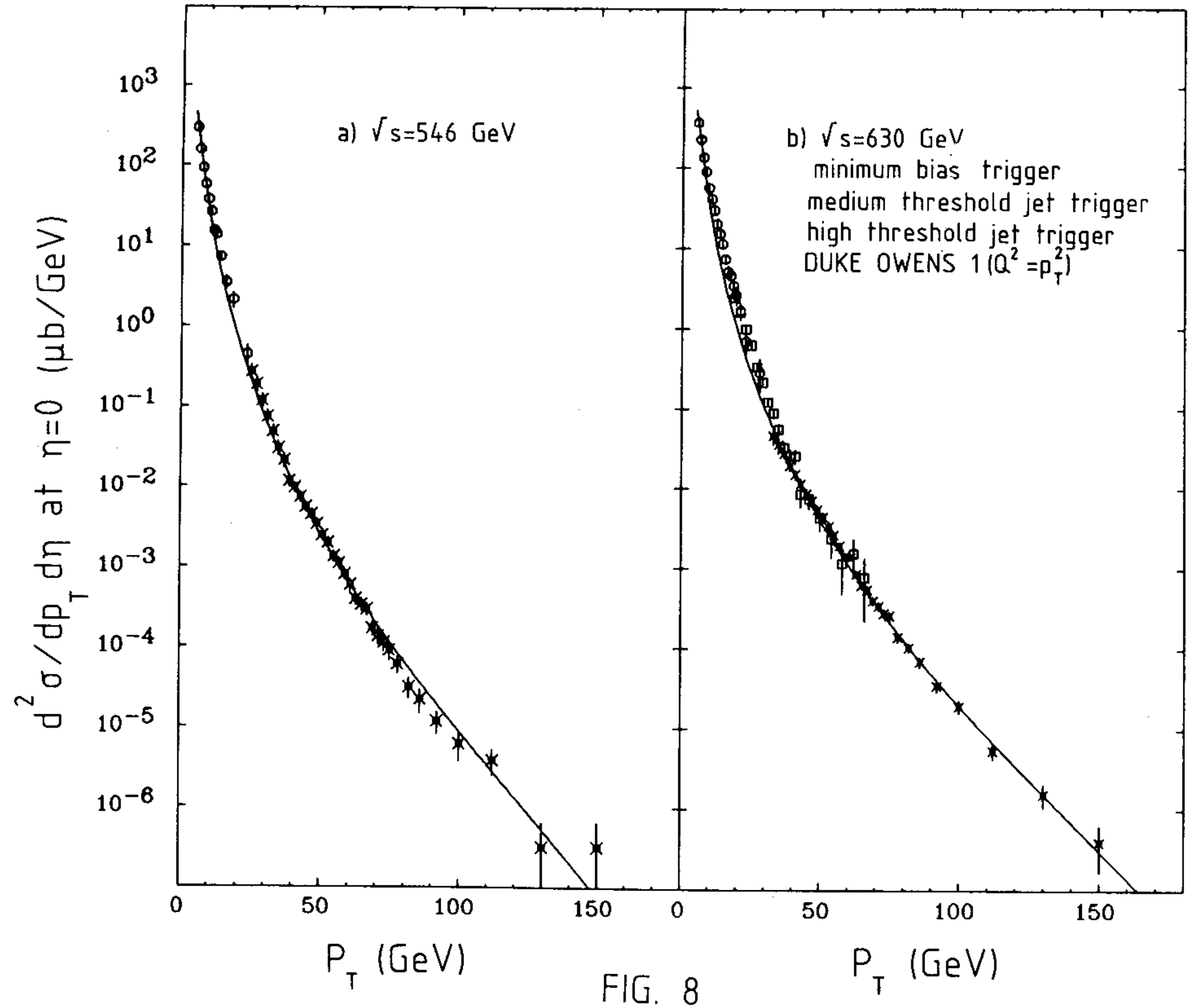

a) √s=546 GeV
b) √s=630 GeV
minimum bias trigger
medium threshold jet trigger
high threshold jet trigger
DUKE OWENS 1 (Q² = p_T²)
d²σ/dp_T dη at η=0 (μb/GeV)
P_T (GeV)

FIG. 8

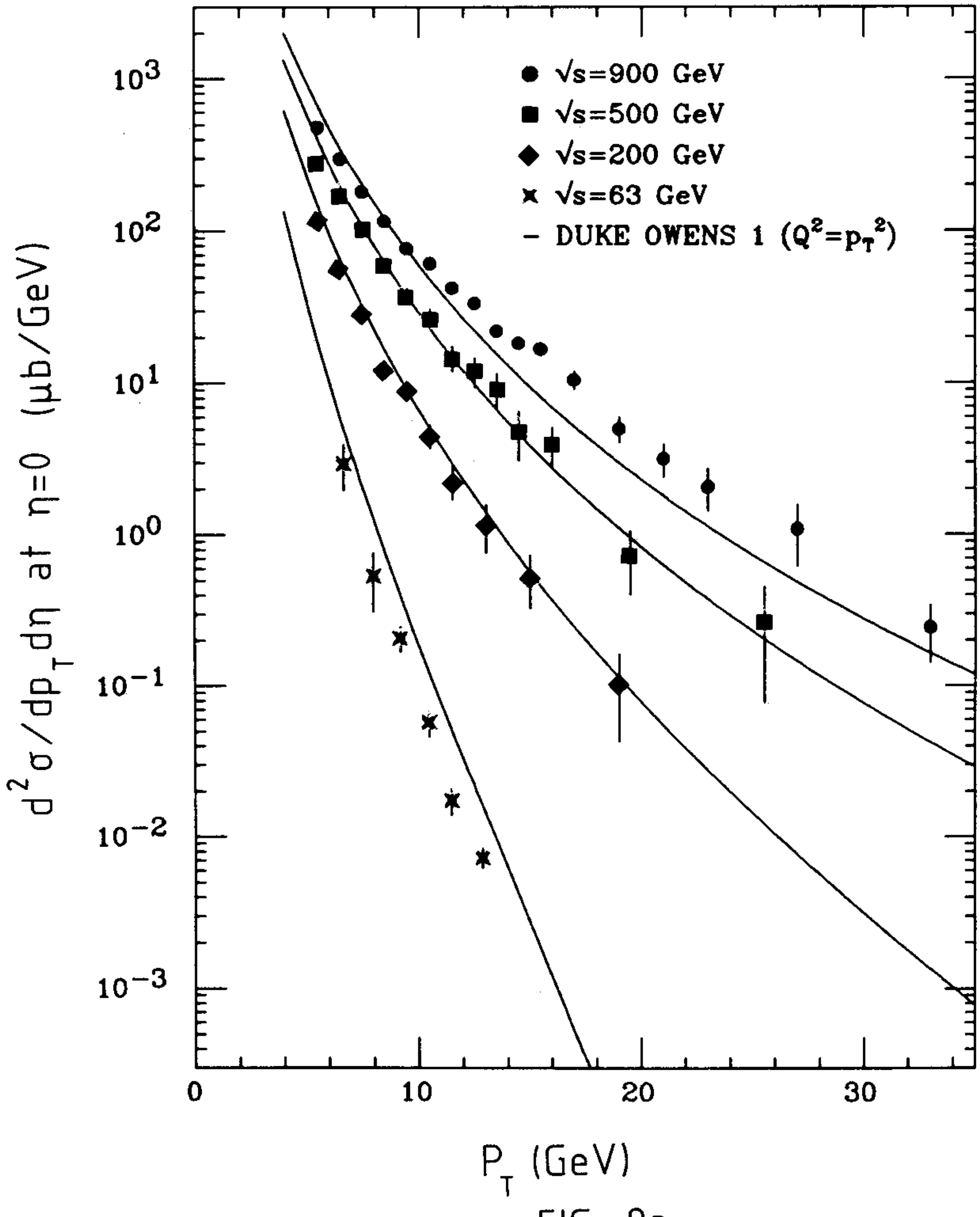

√s=900 GeV
√s=500 GeV
√s=200 GeV
√s=63 GeV
- DUKE OWENS 1 (Q²=p_T²)
d²σ/dp_T dη at η=0 (μb/GeV)
10³
10²
10¹
10⁰
10⁻¹
10⁻²
10⁻³
0
10
20
30
P_T (GeV)

FIG. 9a

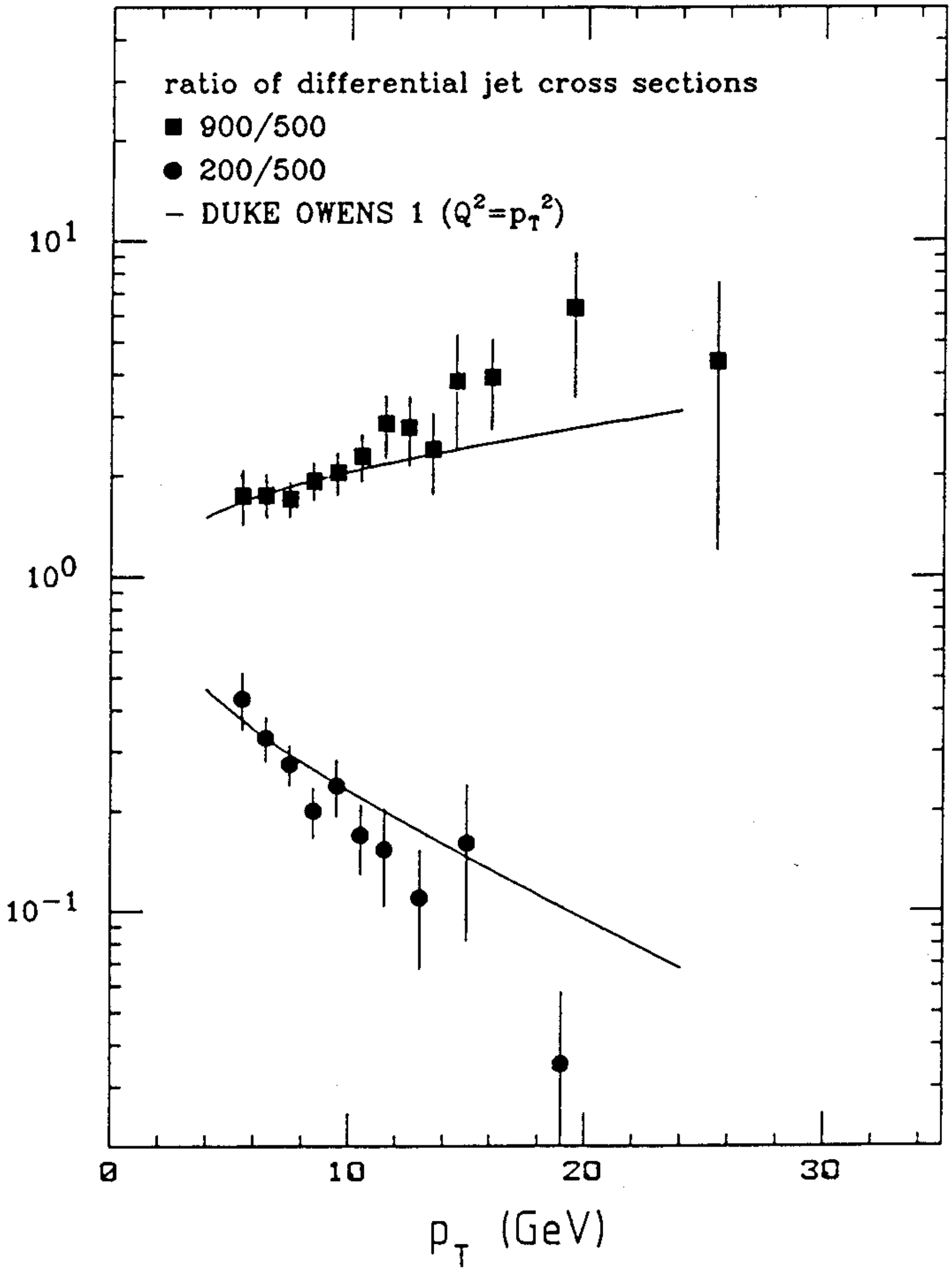

ratio of differential jet cross sections
900/500
200/500
– DUKE OWENS 1 ($Q^2=p_T^2$)
10^1
10^0
10^{-1}
0
10
20
30
p_T (GeV)

FIG. 9b

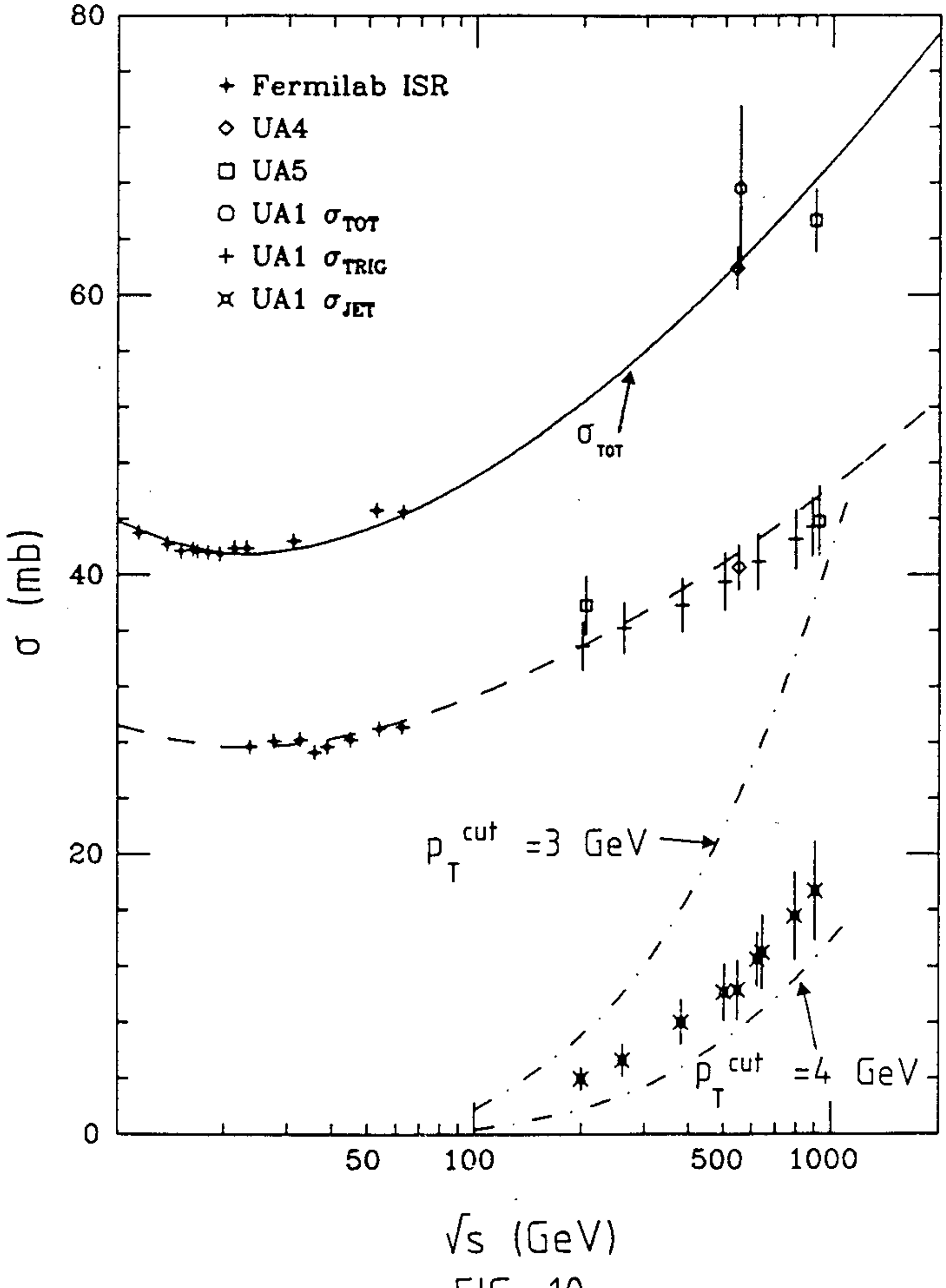

Fermilab ISR
UA4
UA5
UA1 σ_{TOT}
UA1 σ_{TRIG}
UA1 σ_{JET}
σ_{TOT}
p_T^{cut} =3 GeV
p_T^{cut} =4 GeV
σ (mb)
√s (GeV)

FIG. 10